ЖУРНАЛ СТРУКТУРНОЙ ХИМИИ

2011. Том 52, № 5 *Сентябрь – октябрь* *С. 939 – 945*

UDC 548.73:543.422:541.45

VAPOUR PHASE DIFFUSION OF AMMONIA ON THE FIRST ROW TRANSITION METAL SERIES AND ITS EFFECT ON THE CRYSTALLIZATION PROCESS: A STRUCTURAL INVESTIGATION

© 2011 **T.N. Ramesh***

Department of Chemistry, Central College Campus, Bangalore University, Bangalore, India

Received February, 14, 2009

The diffusion of ammonia vapors to the magnesium/manganese/nickel nitrate solution results in the formation of their respective metal hydroxides, while the diffusion of ammonia vapors to copper and zinc nitrate solutions results in the crystallization of layered hydroxysalts. The PXRD patterns show that highly crystalline phases of samples are obtained. Infrared spectra were used to get information on the local coordination of ions. The thermogravimetric analysis justifies the phases concluded from powder X-ray diffraction and infrared spectroscopy. This clearly demonstrates that the crystal structure is mainly dictated by the nature of the metal ion, its site selectivity and specificity under identical synthesis conditions.

K e y w o r d s: diffusion, layered compounds, structure determination.

INTRODUCTION

The crystal structure of cationic clays comprises stacking of negatively charged aluminosilicate layers, with alkali and alkaline earth metal ions in the interlayer region for charge neutrality [1]. These cationic clays are used as sorbents, catalytic supports and in ion exchange reactions [2—4]. It is easier to design and synthesize anionic clays with the properties exactly inverse to those of cationic clays, such as anion exchange, surface basicity, sorbents, etc. [5—7]. Anionic clays derive their structure from mineral brucite [$Mg(OH)_2$]. The crystal structure of magnesium hydroxide consists of hexagonal close packing of hydroxyl ions, in which every alternate layer of the octahedral site is occupied by Mg^{2+} ions. This leads to stacking of charge-neutral hydroxide layers, held together by van der Waals interactions [8]. Such a structure throws light on the possibility of synthesizing layered metal hydroxides and hydroxy salts, layered double hydroxides, oxide-hydroxides, and trivalent metal hydroxides [9, 10]. The physical properties of these compounds are affected by their structure, composition, and morphological features. There are numerous methods to prepare the above mentioned compounds, but the limitation is to control the nature of the reaction [13—15].

Thermodynamic and kinetic factors control the phase formation and crystallinity of these compounds. Ordered crystalline phases of metal hydroxides are generally obtained by an energy intensive hydrothermal technique, thereby controlling the thermodynamic parameter [16]. De Hann obtained single crystals of metal hydroxides and metal hydroxysalts by a simple vapor phase diffusion method at 25—30 °C [17]. Inspired by biological mechanisms in nature, Schwenzer et al. synthesized thin films of highly ordered crystalline hydroxysalts of cobalt, copper, and zinc [18]. They also prepared zinc oxide and manganese phosphate thin films using the vapor phase diffusion method [19]. To the best of our knowledge, there are no reports correlating the changes in the crystal structure, chemical composition, and morphological features based on the property of the metal ion. Using the interdiffusion method, we were able to synthesize layered metal hydroxides and layered hydroxysalts with different chemical compositions using the acidic property of the cation under ambient conditions (25—30 °C).

* E-mail: adityaramesh77@yahoo.com

EXPERIMENTAL

Inter-diffusion method. The diffusion of ammonia vapors to the required metal nitrate solution results in the formation of highly crystalline compounds. A metal nitrate solution (2 M; 15.4 ml) [$M^{2+} = Mg(NO_3)_2$] was added by means of a pipette to a 100 ml beaker containing 75 ml of water. This solution together with aqueous ammonia (2 M, 150 ml) in a separate beaker was placed in a vacuum glass desiccator. After 2 days, the precipitated compound settled down at the bottom of the beaker. After 5 days, a fresh aliquot of aqueous ammonia was replaced and the reaction was allowed to continue further. At the end of the 8th day, pH of the metal nitrate solution was around 9. Using the above procedure, a series of compounds were obtained with different metal nitrate solutions (Co, Ni, Cu, Zn, and Cd) at 25—30 °C.

In the case of nickel, the blue nickelammine complex was formed in addition to a green precipitate of nickel hydroxide. For cobalt ions, single crystals of the cobalt hexamine complex formed. The precipitates obtained in all these cases are not quantitative.

CHARACTERIZATION

All the samples were characterized by PXRD using a Siemens D5005 diffractometer with a CuK_α (λ = 1.5418 Å) source. IR spectra were obtained using a Nicolet Model Impact 400D FTIR spectrometer (KBr pellets, resolution 4 cm^{-1}). Thermogravimetric analysis of all the samples was carried out using a Mettler Toledo Model 850e TG/SDTA system (heating rate 5 °C/min). The metal content was determined by weighing the final products obtained (MgO, NiO, CuO, ZnO, CdO) after thermal decomposition at 700 °C. SEM images were recorded using a SIRON electron microscope. Rietveld refinement was carried out on the crystal structure of the samples using the Fullprof program to compare it with standard samples [20].

RESULTS AND DISCUSSION

The solid obtained immediately on precipitation is not only highly disordered, but also thermodynamically unstable with a free energy close to that of the reactants [21]. The disordered phase transforms into a more stable phase by lowering the free energy in a step-wise manner. The factors that can affect the product formation are: (i) conditions under which experiments are carried out; (ii) reaction path taken during the transformation to thermodynamically stable phases and (iii) charge and size of the metal ion. The charge of the metal ion is directly proportional to the acidity of the metal ion, while when the metal ion size decreases, the metal ion acidity decreases.

The diffusion process provides an opportunity to control the kinetics of the reaction thereby allowing the crystal growth. Metal nitrate solutions are acidic in nature with pH around 1—3. During the diffusion process, ammonia vapors dissolve in water forming ammonium hydroxide

$$NH_3(v) + H_2O(l) \rightarrow NH_4^+ + OH^-.$$

On a prolonged exposure, the hydroxide ion concentration increases in the metal nitrate solution. When the solubility product (K_{sp}) of the metal ion exceeds, the metal ion precipitates as its respective hydroxide/oxyhydroxide/hydroxysalt [22]. Table 1 lists the solubility product of all the metal ions.

Table 1

Solubility product of various metal hydroxides at 25 °C

Compound	Solubility product (K_{sp})
$Mg(OH)_2$	$3 \cdot 10^{-34}$
$Ni(OH)_2$	$5.48 \cdot 10^{-16}$
$Co(OH)_2$	$5.92 \cdot 10^{-15}$
$Mn(OH)_2$	$5.6 \cdot 10^{-12}$
$Cd(OH)_2$	$7.2 \cdot 10^{-15}$

The diffusion of ammonia vapors to the nickel nitrate solution results in the formation of a blue-colored nickelammine complex. Slow hydrolysis of the nickel ammine complex results in the formation of nickel hydroxide. The overall reaction can be expressed as follows:

$$Ni(NO_3)_2 + 6\ NH_4(OH) \Leftrightarrow [Ni(NH_3)_6]^{2+} + 6\ H_2O + 2\ OH^-$$

$$[Ni(NH_3)_6]^{2+} \Leftrightarrow Ni^{2+} + 6\ NH_3$$

$$6\ NH_3 + 6\ H_2O \Leftrightarrow 6\ NH_4(OH).$$

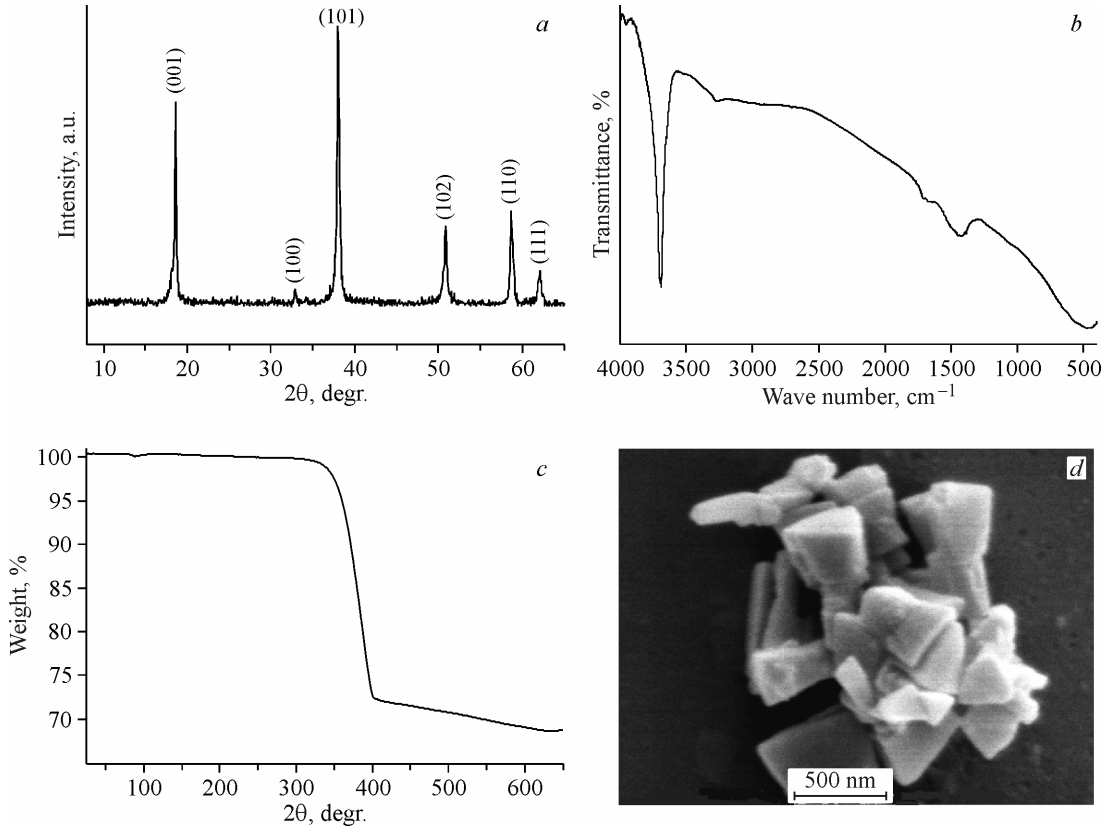

Fig. 1. (*a*) Rietveld refinement of the PXRD pattern of magnesium hydroxide, (*b*) IR spectrum, (*c*) thermogram, and (*d*) SEM of magnesium hydroxide

The amphoteric nature of nickel hydroxide allows it to precipitate as nickel hydroxide

$$Ni^{2+} + 6\ NH_4(OH) \Leftrightarrow \beta\text{-}Ni(OH)_2.$$

Polycrystalline samples are obtained in contrast to single crystals obtained by de Hann. In the case of a magnesium nitrate precursor, the precipitation takes place immediately without any intermediate stages.

Figs. 1, *a* and 2, *a* show the PXRD patterns of magnesium and nickel hydroxides obtained by the diffusion of ammonia vapors to magnesium and nickel nitrate solutions respectively. The reflections in the PXRD patterns of magnesium and nickel hydroxides match well with the mineral brucite structure having interlayer spacings of 4.7 Å (ICSD 89823) and 4.6 Å (ICSD 28101) respectively. Rietveld refinement was carried out on the PXRD patterns of magnesium and nickel hydroxide samples to characterize the crystalline nature of the compounds (see open circles in Figs. 1, *a* and 2, *a*).

The IR spectrum of magnesium hydroxide shows two absorptions: (i) a 3698 cm^{-1} peak due to non-hydrogen bonded OH groups and (ii) Mg—O stretching at 468 cm^{-1} (Fig. 1, *b*). The IR spectrum of nickel hydroxide also displays the features similar to that of nickel hydroxide (data not provided). Figs. 1, *c* and 2, *b* show the thermograms of magnesium and nickel hydroxides respectively. Magnesium hydroxide shows single step weight loss of 25.6 %, while nickel hydroxide shows 17.6 % weight loss. In both cases, the decomposed products are MgO and NiO. Figs. 1, *d* and 2, *c* show the SEM images of magnesium and nickel hydroxides respectively. They reveal the platelet type of morphologies.

The diffusion of ammonia vapors to the cobalt nitrate solution produces orange colored single crystals. These single crystals dissolve immediately on washing with water indicating it to be the hexamine cobalt(II) nitrate complex. The usage of a concentrated cobalt nitrate solution tends to form the hexamine cobalt complex. Schewenzer and coworkers obtained thin films of cobalt hydroxysalts by the diffusion of ammonia vapors to the cobalt nitrate solution at a lower concentration [18].

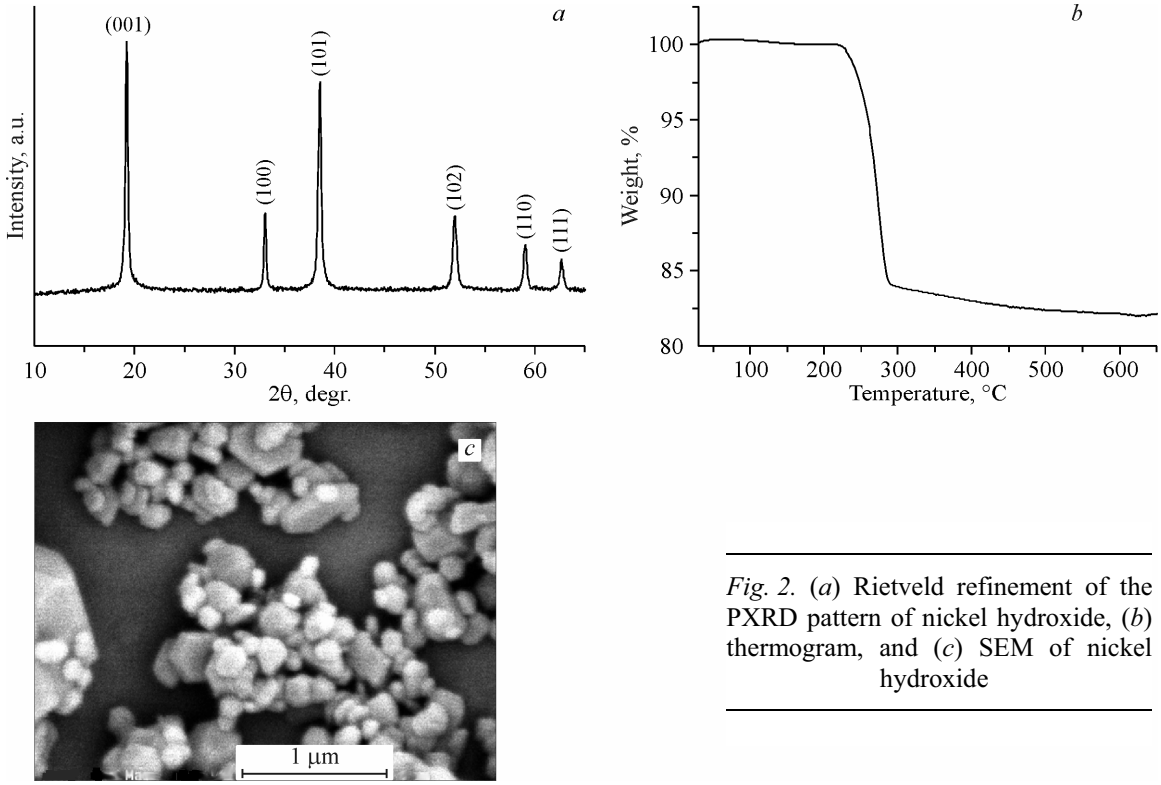

Fig. 2. (*a*) Rietveld refinement of the PXRD pattern of nickel hydroxide, (*b*) thermogram, and (*c*) SEM of nickel hydroxide

Fig. 3, *a* shows the PXRD pattern of copper hydroxynitrate obtained by the diffusion of ammonia vapors to the copper nitrate solution. The reflections in the PXRD pattern of copper hydroxynitrate match with those of $Cu_2(OH)_3NO_3$ (ICSD 31353). Rietveld refinement was carried out on the PXRD pattern of copper hydroxynitrate (see open circles in Fig. 3, *a*). The PXRD pattern of the product obtained by the diffusion of ammonia vapors to the zinc nitrate solution matches well with that of $Zn_5(OH)_8(NO_3)_2 \cdot 2H_2O$ (ICSD 16023, Fig. 4, *a*). $Cu_2(OH)_3NO_3$ and $Zn_5(OH)_8(NO_3)_2 \cdot 2H_2O$ are generally considered as layered hydroxysalts, which also derive their structure from brucite mineral. The structure of layered hydroxysalt comprises stacking of hydroxyl deficient positively charged layers having the composition $[M(OH)_{2-x}]^{x+}$. The coordinative unsaturation of the metal ion is satisfied by the anion that grafts directly to the metal ion yielding compounds with the general formula $[M(OH)_{2-x}]^{x+} \times \times (A^{n-})_{x/n}$ [9]. The interlayer spacing between the metal hydroxide layers is mainly determined by the anion size and usually varies from 6.9 to 9.2 Å [23, 24]. Cu^{2+} prefers to crystallize as a layered hydroxysalt instead of a hydroxide due to the Jahn—Teller distortion. The Zn^{2+} ion can occupy both octahedral and tetrahedral sites forming a monoclinic structure by decreasing the free energy of the crystal.

In $Cu_2(OH)_3NO_3$, Cu^{2+} ions occupy two different crystallographic positions with the first Cu^{2+} ion being coordinated by four OH groups and two oxygens of NO^{3-}, while the second Cu^{2+} ion is coordinated by four OH^- anions in the plane and one OH^- other oxygen from the NH_3^- [11]. $Zn_5(OH)_8(NO_3)_2 \cdot 2H_2O$ can be formulated as $[Zn_{octa3}Zn_{tetra2}(OH)_8][NO_3]_2 \cdot 2H_2O$, where $x = 0.25$. The structure consists of $[Zn_3(OH)_8]^{2-}$ layers with $x = 0.25$ of the octahedral positions being unoccupied. Above and below the unoccupied octahedral positions, two zinc ions occupy tetrahedral positions. The coordination of tetrahedra around zinc is completed by the contribution of oxygen atoms from water molecules and the nitrate ion [25].

The IR spectrum of copper hydroxynitrate shows broad peaks in the region of 3547 cm^{-1} and 3429 cm^{-1} due to OH^- stretching and hydrogen bonded OH^- vibrations. Peaks observed in the region of 800—400 cm^{-1} are due to δ(Cu—O—H) (677 cm^{-1}) and (Cu—O) (457 cm^{-1}) vibrations, whereas peaks due to the nitrate groups are in the 1600—1000 cm^{-1} region. Copper hydroxynitrate shows three strong absorptions (ν_1: 1347 cm^{-1}; ν_2: 1048 cm^{-1}, and ν_4: 1423 cm^{-1}) assigned to the strongly bound

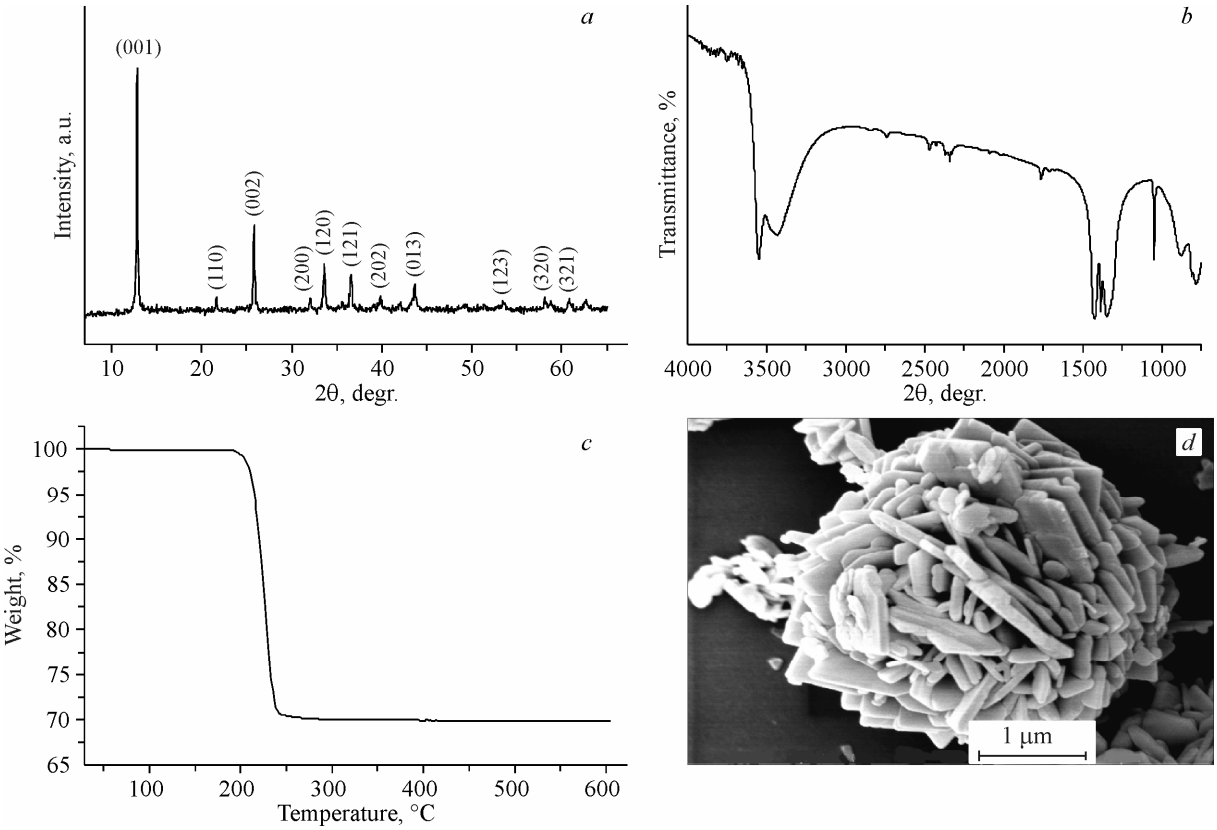

Fig. 3. (*a*) Rietveld refinement of the PXRD pattern of copper hydroxynitrate, (*b*) IR spectrum, (*c*) thermogram, and (*d*) SEM of copper hydroxynitrate

nitrate group. A large splitting $\Delta\nu = 76$ cm^{-1} between the ν_4 and ν_1 vibrational modes of the nitrate ion in the IR spectrum of copper hydroxynitrate provides a direct evidence for grafting one of the oxygen atoms of the nitrate to the metal atom to complete the octahedral coordination around the metal ion via covalent bonding [26]. This will lower the free energy of the crystal by minimizing the enthalpy due to the completion of the first coordination shell. In this coordination mode, one of the C_2 axes (N—O) of the nitrate ion is parallel to the *c* crystallographic axis [27]. The IR spectrum of $Zn_5(OH)_8(NO_3)_2 \cdot \cdot 2H_2O$ shows the hydroxyl stretch at 3433 cm^{-1}. The presence of the nitrate ion coordinated to the layer is revealed by the split of a single band to 1512 cm^{-1}, 1417 cm^{-1}, and 1384 cm^{-1} respectively. Fig. 3, *c* shows the thermogravimetric data of copper hydroxynitrate. Copper hydroxynitrate decomposes in a single step at 290 °C. Deanation and dehydroxylation take place simultaneously leading to the formation of CuO. In Figs. 3, *d* and 4, *c* are shown the SEM images of $Cu_2(OH)_3(NO_3)$ with the hexagonal platelet-like morphology and $Zn_5(OH)_8(NO_3)_2 \cdot 2H_2O$ with the sheet-like morphology respectively.

The PXRD pattern of the product obtained by the diffusion of ammonia vapors to the manganese nitrate solution is X-ray amorphous (data not shown). Thermogravimetric data of the product obtained by the diffusion of ammonia vapors to the manganese nitrate solution show the total weight loss (14.2 %). This weight loss matches with the expected weight loss for manganese hydroxide (14.25 %). The IR spectrum of manganese hydroxide exhibits a broad peak at 3343 cm^{-1} due to O—H stretching. Peaks at 1633 cm^{-1}, 607 cm^{-1}, and 498 cm^{-1} are due to water bending, M—O—H, and M—O stretching vibrations respectively.

The PXRD pattern of the compound obtained by the diffusion of ammonia vapors to the cadmium nitrate solution results in the formation of a biphasic mixture of CdO and $Cd(OH)_2$. Table 2 gives the hydrolysis constants (*K*) and precipitation pH (at 25 °C) for various metal nitrate solutions.

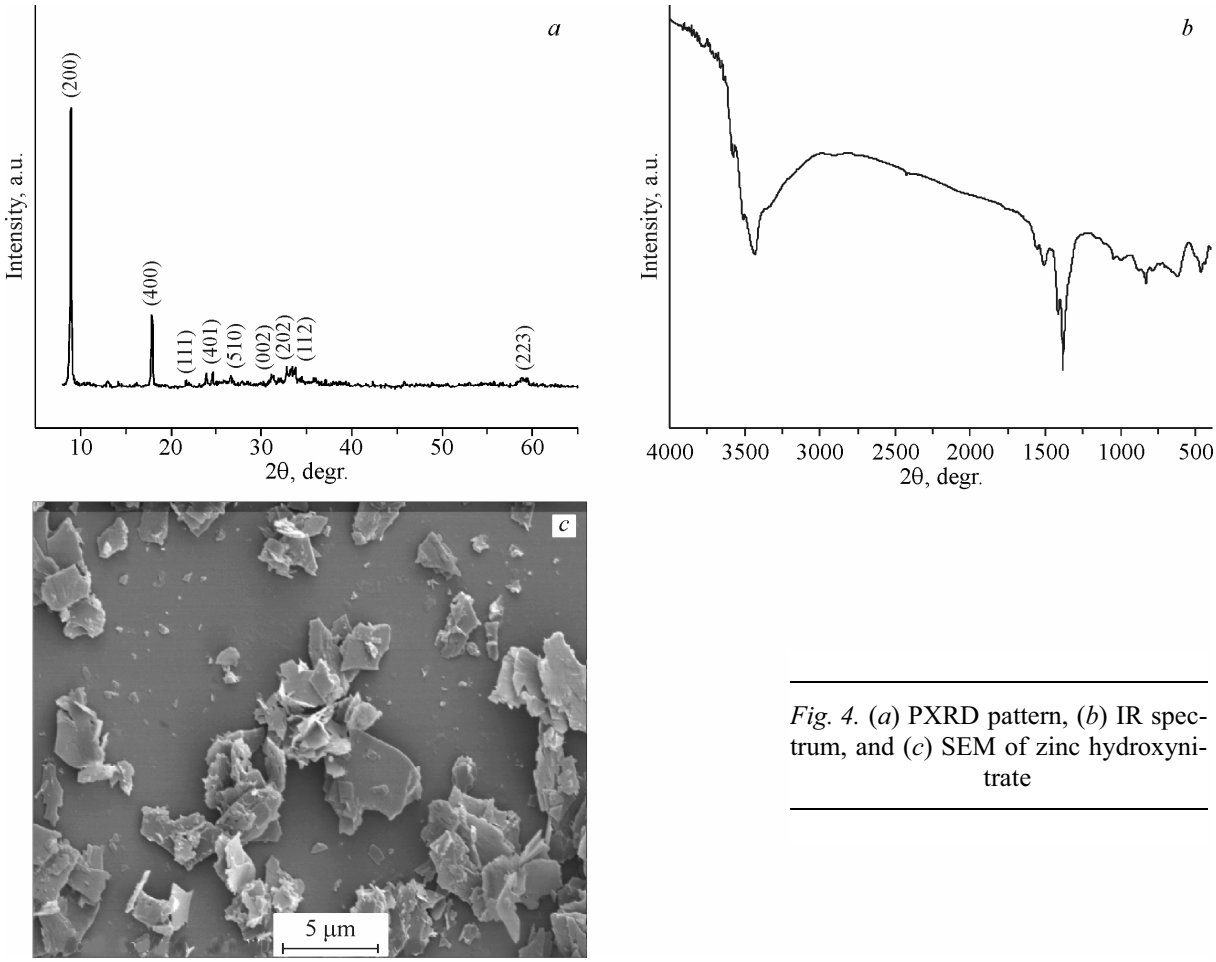

Fig. 4. (*a*) PXRD pattern, (*b*) IR spectrum, and (*c*) SEM of zinc hydroxynitrate

Hence, when we move from left to right in the periodic table of the transition metal series (Fe to Zn), the acidity of the metal ion decreases and the structure of the compound changes.

Magnesium, nickel, and manganese nitrate solutions precipitate as their respective metal hydroxides, whereas copper and zinc nitrate solutions are at the end of the transition metal series with less acidity leading to the formation of their respective hydroxysalts. These layered hydroxysalts are intermediate phases between metal nitrate and metal hydroxide. The copper ion acidity is slightly higher than that of the zinc ion resulting in changes in the chemical composition within the class of layered hydroxysalts. The copper ion prefers octahedral coordination, while the zinc ion can occupy both octahedral and tetrahedral sites due to a smaller ionic radius. Thus, the structure and chemical composition of these compounds are mainly dictated by (i) the size, (ii) site selectivity, and (iii) the nature of the metal ion.

T a b l e 2

Hydrolysis constants for $M^{n+} + H_2O \Leftrightarrow MOH^{(n-1)+} + H^+$ *with the precipitation* pH *as their respective hydroxides*

Metal ion	*K*	pH
Fe(III)	–2.4	2.0
Mn(II)	–10.6	8.0
Ni(II)	–10.5	8.0
Cu(II)	–8.0	6.0
Zn(II)	–9.1	7.0
Mg(II)	–10.5	8.0

CONCLUSIONS

We have synthesized layered materials that display diverse crystal structures, chemical compositions, and morphologies. The crystal structure is mainly controlled by packing of hydroxyl ions derived from mineral brucite. When all the crystallographically defined anion sites in the hydroxide layers are occupied by hydroxyl ions, the compounds can be referred to as hydroxides [$Mg(OH)_2$ and $Ni(OH)_2$]. When some of the crystallographically defined sites in the hydroxide layers are occupied by nitrate ions, which are grafted to the metal, then the compounds can be referred to as basic salts. The

structure is also dictated by the size and site specificity of the metal ion. In conclusion, the mechanisms of generating anionic clays, hydroxides, and hydroxysalts are dictated by the property of the cation.

Acknowledgements. TNR thanks the Council of Scientific and Industrial Research, GOI for the award of a Senior Research Fellowship (NET) and Research Associate (RA). Author thanks P Vishnu Kamath, Bangalore University for providing laboratory facilities and Solid State and Structural Chemistry Unit, Indian Institute of Science for powder X-ray diffraction facilities.

REFERENCES

1. *McCabe R.W.* Inorganic Materials / Eds. D.W. Bruce, D. O′Hare. – New York: John Wiley, Sons, 1992.
2. *Keren R.* // Clays Clay Miner. – 1986. – **34**, N 5. – P. 534 – 538.
3. *Loeppert R.H., Zelazny L.W., Volk B.G.* // Clays Clay Miner. – 1986. – **34**, N 1. – P. 87 – 92.
4. *Fan C., Zhuang Y., Li G.et al.* // Electro Analysis. – 2000. – **12**, N 14. – P. 1156 – 1158.
5. *Ookkubo A., Ooi K., Hayashi H.* // Langmuir. – 1993. – **9**, N 5. – P. 1418 – 1422.
6. *Reichle W.T.* // J. Catal. – 1985. – **94**, N 2. – P. 547 – 557.
7. *Kamath P.V., Dixit M., Indira L. et al.* // J. Electrochem. Soc. – 1994. – **141**, N 11. – P. 2956 – 2959.
8. *Oswald H.R., Asper R.* / Preparation, Crystal Growth of Materials with Layered Structure / Ed. R.M.A. Leith, Riedel Publishing Company. – Netherlands, 1977.
9. *Cavani F., Trifiro F., Vaccari A.* // Catal. Today. – 1991. – **11**, N 2. – P. 173 – 301.
10. *Wells A.F.* Structural Inorganic Chemistry. – Oxford: Oxford University Press, 1979.
13. *Grosso R.P., Suib S.L., Weber R.S., Schubert P.F.* // Chem. Mater. – 1992. – **4**, N 4. – P. 922 – 928.
14. *Braconnier J.J., Delmas C., Fouassier C. et al.* // Rev. Chim. Miner. – 1984. – **21**. – P. 496 – 499.
15. *De Voreo J.J., Vekilov P.G.* Reviews in Minerology, Geochemistry, Minerological Society of America / Eds. P.M. Dove, J.J. De Voreo, S. Weiner. – Washington: DC, 2004.
16. *Rabenau A.* // Angew. Chem. Int. Ed. Engl. – 1985. – **24**, N 12. – P. 1026 – 1040.
17. *De Hann Y.M.* // Nature. – 1963. – **200**, N 4909. – P. 876 – 924.
18. *Schwenzer B., Roth K.M., Gomm J.R. et al.* // J. Mater. Chem. – 2006. – **16**, N 4. – P. 401 – 407.
19. *Kisailus D., Kisailus B., Schwenzer J. et al.* // J. Amer. Chem. Soc. – 2006. – **128**, N 31. – P. 10276 – 10280.
20. *Rodriguez-Carvajal J.* ″FULLPROF: A Program for Rietveld Refinement, Pattern Matching Analysis″, Abstracts of the Satellite Meeting on Powder Diffraction of the XV Congress of the IUC, Toulouse, France, 1990.
21. *Ostwald W.* // Z. Physik. Chem. – 1897. – **22**. – S. 289, as quoted in ref. 12.
22. *Dobos D.* Electrochemical Data: A Handbook for Electrochemists in Industry, Universities. – Amsterdam: Elsevier, 1975.
23. *Meyn M., Beneke K., Lagaly G.* // Inorg. Chem. – 1993. – **32**, N 7. – P. 1209 – 1215.
24. *Nishizawa H., Markov L., Ioncheva R.* // J. Mater. Sci. Lett. – 1998. – **14**. – P. 290 – 295.
25. *Stahlin W., Ostwald H.R.* // Acta Crystallogr. – 1970. – **26**, N 3. – P. 860 – 863.
26. *Portemer F., Delahaye-Viadal A., Figlarz M.* // J. Electrochem. Soc. – 1992. – **139**, N 3. – P. 671 – 678.
27. *Ross S.D.* Inorganic Infrared, Raman Spectra. – London: McGraw-Hill, 1972.